



A EUROPEAN JOURNAL OF CHEMICAL BIOLOGY

CHEM **BIO** CHEM

SYNTHETIC BIOLOGY & BIO-NANOTECHNOLOGY

Accepted Article

Title: In silico evaluation of the binding site of fucosyltransferase 8 and first attempts of synthesizing an inhibitor with drug-like properties

Authors: Claas Strecker, Melissa Baerenfaenger, Michaela Mieke, Edzard Spillner, and Bernd Meyer

This manuscript has been accepted after peer review and appears as an Accepted Article online prior to editing, proofing, and formal publication of the final Version of Record (VoR). This work is currently citable by using the Digital Object Identifier (DOI) given below. The VoR will be published online in Early View as soon as possible and may be different to this Accepted Article as a result of editing. Readers should obtain the VoR from the journal website shown below when it is published to ensure accuracy of information. The authors are responsible for the content of this Accepted Article.

To be cited as: *ChemBioChem* 10.1002/cbic.201900289

Link to VoR: <http://dx.doi.org/10.1002/cbic.201900289>

WILEY-VCH

www.chembiochem.org

A Journal of



In silico evaluation of the binding site of fucosyltransferase 8 and first attempts of synthesizing an inhibitor with drug-like properties

Claas Strecker,^[a] Melissa Baerenfaenger,^[a,b] Michaela Mieke,^[c] Edzard Spiller,^[c] and Bernd Meyer^{*[a]}

Abstract: Core fucosylation of *N*-glycans is catalyzed by fucosyltransferase 8 and is associated with various types of cancer. Most reported fucosyltransferase inhibitors carry non drug-like features, like charged groups. New starting points for development of inhibitors of fucosyltransferase 8 are presented using a fragment-based strategy. First, we discuss the potential of a new putative binding site of fucosyltransferase 8 that becomes accessible by a significant motion of the SH3-domain according to an MD simulation. This might enable design of completely new inhibitor types for fucosyltransferase 8. Second, we performed a docking campaign against the donor binding site of fucosyltransferase 8 yielding two fragments that were linked and trimmed *in silico*. The resulting ligand was synthesized. STD NMR confirmed binding of the ligand with a pyrazole core that mimics the guanine moiety. This low affinity ligand represents the first low-molecular weight molecule for development of inhibitors of fucosyltransferase 8 with drug-like properties.

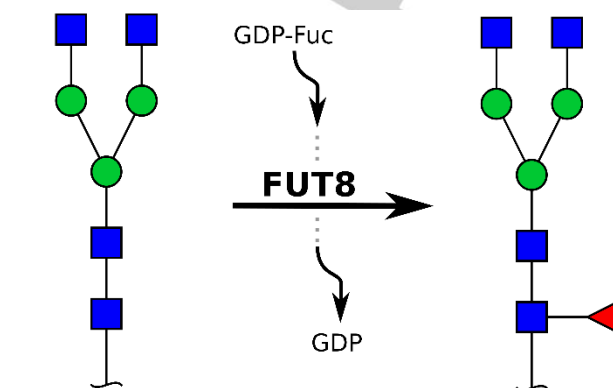


Figure 1. Fucosyltransferase 8 (FUT8) catalyzes the transfer of a fucose moiety from the donor substrate GDP-Fucose onto the 6-OH group of innermost *N*-acetylglucosamine of the acceptor *N*-glycan yielding a core fucosylated *N*-glycan.

Introduction

Fucosyltransferases catalyze the transfer of fucose from the donor substrate GDP-Fucose onto an acceptor glycan. The human genome encodes 13 fucosyltransferases (FUT1-11 and POFUT1-2). Even though they show distinct substrate preferences, a certain degree of redundancy exists. For example FUT1 and FUT2 both yield α 1,2-linked fucose and both are able to act on *O*- as well as on *N*-glycans.¹ In contrast, fucosyltransferase 8 (FUT8) is the only fucosyltransferase that aids the construction of α 1,6-linked fucose and that acts exclusively on *N*-glycans.¹ The enzyme transfers fucose to the innermost *N*-acetyl glucosamine of *N*-glycans, resulting in core fucosylation (cf. Fig. 1).

For therapeutic antibodies, it has been shown that depletion of core fucosylation results in a 50-100 fold increase of Fc γ -mediated cytotoxicity.² As a result, methods for the production of non-fucosylated antibodies are of significant commercial interest. Functional disruption of FUT8 in CHO cell lines has previously been achieved by the use of zinc-finger nucleases.³ Furthermore, core fucosylation has been implicated to play a role in various types of cancer. For example, upregulation of FUT8 is a driver of melanoma metastasis,⁴ associated with an unfavourable clinical outcome in patients with non-small cell lung cancer,⁵ and with aggressive prostate cancer.⁶ The important physiological role of FUT8 is underlined by the fact that 70% of FUT8-deficient knock-out mice die within three days after birth.⁷ Inhibitors of FUT8 would therefore constitute an efficient tool for more detailed studies on the physiological role of FUT8 and might demonstrate therapeutic potential as well.

Development of glycosyltransferase inhibitors has been held back by a ubiquitous focus on substrate analogues.⁸ Analogues of the donor substrate offer easily reachable binding affinity as the phosphate group(s) of the donor substrate account for a major portion of the binding affinity. Analogues of the acceptor substrate offer a level of specificity that would be very tedious to achieve otherwise. However, these close substrate analogues have limited potential because they typically feature non drug-like properties, e.g. a high polarity, that diminish their cell viability as formulated in Lipinski's rule of five.⁹ Specifically, previous statements apply for fucosyltransferase inhibitors as well (see the review by Tu *et al.*).¹⁰ To circumvent the problems that are associated with inhibitors, which feature non drug-like properties, we have embraced a fragment-based strategy for the development of inhibitors of FUT8 that allows for more control over molecular properties.

[a] M. Sc. C. Strecker, M. Sc. M. Baerenfaenger, Prof. Dr. B. Meyer
Department of Chemistry
University of Hamburg
Martin-Luther-King-Platz 6, 20146 Hamburg, Germany
E-mail: bernd.meyer@chemie.uni-hamburg.de

[b] Present address:
Department of Neurology
Radboud University Medical Center
Geert Grooteplein 10, Nijmegen, 6525 GA, The Netherlands

[c] Dr. M. Mieke, Prof. Dr. E. Spillner
Department of Engineering
Aarhus University
Gustav Wieds Vej 10, 8000 Aarhus, Denmark

Supporting information for this article is given via a link at the end of the document.

So far, three publications have reported inhibitors of FUT8.¹¹⁻¹³ Manabe *et al.*¹¹ and Hosoguchi *et al.*¹² reported analogues of GDP-Fucose that inhibit FUT8. Their most potent inhibitors (as shown in supplemental Fig. S1) exhibit affinities in the lower μM range. However, the corresponding clogP values of less than -1.5 indicate that bioavailability is not present or extremely low. Kamińska *et al.* reported a set of triazine dyes that inhibits FUT8.¹³ Their most potent inhibitor reactive red 120 (see supplemental Fig. S1) carries six ionic sulfonates that will prevent membrane permeability. In addition, the molecular mass of more than 1300 Da grossly violates Lipinski's rule. While the reported K_i of 2 μM for reactive red 120 sounds promising on first sight, the concept of ligand efficiency ($\text{LE} = \Delta G/\text{no. of heavy atoms}$)¹⁴ proves that reactive red 120 is a very inefficient binder with a ligand efficiency of only 0.09.

The acceptor substrate preference of FUT8 has been investigated: FUT8 shows its highest conversion rates on the heptasaccharide displayed in Fig. 1.¹⁵ While FUT8 tolerates modifications of the 6-branch, modifications of 3-branch are usually not accepted.¹⁵ A X-ray crystal structure of *apo* FUT8 exists (PDB: 2DE0).¹⁶ On its basis, models of the binding mode of GDP-Fucose and the acceptor *N*-glycan have been developed.¹⁷⁻¹⁸

Results and Discussion

In the absence of potent and selective inhibitors of FUT8, biochemical studies lack an efficient tool to clearly define the physiological role of the product(s) of this enzyme. FUT8 has a binding site that encompasses eight monosaccharide residues (one fucosyl residue and seven monosaccharide building blocks from the acceptor), a purine based nucleoside and a pyrophosphate group. It is very difficult to find molecules that bind to such large binding sites and exert affinity and specificity. Here, we present our approaches to discover inhibitors for FUT8. In a first part, a putative new binding site and its potential is discussed. In a second part, a fragment-based approach is utilized to generate new chemical entities for binders of the donor site.

A Putative Allosteric Binding Site:

An X-ray crystal structure of human FUT8 (PDB: 2DE0) served as the starting point to our structure-based ligand discovery process.¹⁶ This is an *apo* crystal structure and a key catalytic residue (Arg-365) is collapsed into the donor binding site. Therefore, we created a model for donor substrate binding that has previously been developed in our working group.¹⁷ On the basis of this model, we performed a MD simulation of a length of 20 ns to explore the flexibility of FUT8. The analysis of this MD simulation showed evidence of a putative allosteric binding site that will be discussed in the following. Panel A of Fig. 2 displays a matrix of pairwise RMSD values (for all backbone atoms) of structures taken from this MD simulation. The RMSD matrix shows a significant conformational change occurring after approximately 14.4 ns. Because RMSD matrices can be rather

confusing, we used multidimensional scaling (a form of dimensionality reduction)¹⁹ to point out this conformational change (see the lower part of panel A in Fig. 2). Next, we analyzed the origin of the conformational change. For this, for all investigated structures the RMSD (of the $\text{C}\alpha$ -atom) of each residue is calculated in reference to the initial frame of this MD simulation. The resulting data is plotted in panel B of Fig. 2. The plot reveals that the conformational change is caused by residues of the SH3 domain of FUT8 (colored in magenta in the lower part of panel B in Fig. 2). The SH3 domain of FUT8 is located at the C-terminus.¹⁶ SH3 domains are known to play a role in protein-protein interactions, e.g. in signal-transduction networks.²⁰ However, for the SH3 domain of FUT8 no such function has been described so far.¹⁶ Yet, the SH3 of FUT8 is responsible for the accommodation of the 6-branch of the acceptor *N*-glycan.¹⁸ It has been noted previously that FUT8 is significantly more tolerant to modifications of the 6-branch of the acceptor *N*-glycan than to modifications of the 3-branch.¹⁵ The significant flexibility of the SH3 domain observed in this MD simulations can explain this acceptor specificity well. Even more interestingly, the observed movement of the SH3 domain of FUT8 opens a channel (see panel C of Fig. 2) that connects to a putative binding site (cf. Fig. 3 and the next paragraph).

We assessed the druggability of this putative binding site *in silico*. For this we used FTMap, an application for the identification of binding „hot spots“.²¹ Prior work e.g. from Mattos *et al.*, who crystallized proteins in the presence of organic solvent molecules to investigate binding „hot spots“, laid the experimental foundation for *in silico* tools such as FTMap.²² FTMap places small molecular probes (such as acetamide, ethanol, cyclohexane and urea) with varying functionality and size onto the surface of the investigated protein and finds likely binding sites for these probes by the use of energy functions.²¹ The MD-derived structure shown on the right side of panel C in Fig. 2 was taken to FTMap. Interestingly, on the back side (viewing from the acceptor site) of the channel that opens in the described MD simulation four binding „hot spots“ were identified by FTMap (as shown in Fig. 3). These four „hot spots“ accommodate a total of 45 probe molecules (see supplemental Tab. S1 for a list). In comparison, for the donor binding site of FUT8 (of the same MD-derived structure) FTMap identified four „hot spots“ as well. However, these accommodate only a total of 23 probe molecules. This indicates that this putative binding site might be druggable. A ligand binding to this putative binding site and extending into the channel towards the acceptor binding site might lock this conformation of the acceptor site and therefore alter the acceptor preferences of FUT8. A ligand that extends even further from the channel into the acceptor binding site could possibly disrupt the enzymatic activity of FUT8. Additionally, ligands of this putative binding site might offer specificity over other fucosyltransferases. In contrast, ligands that target the donor binding site of FUT8 will likely also inhibit other fucosyltransferases as all of them use GDP-Fucose as a donor substrate.

For internal use, please do not delete. Submitted_Manuscript

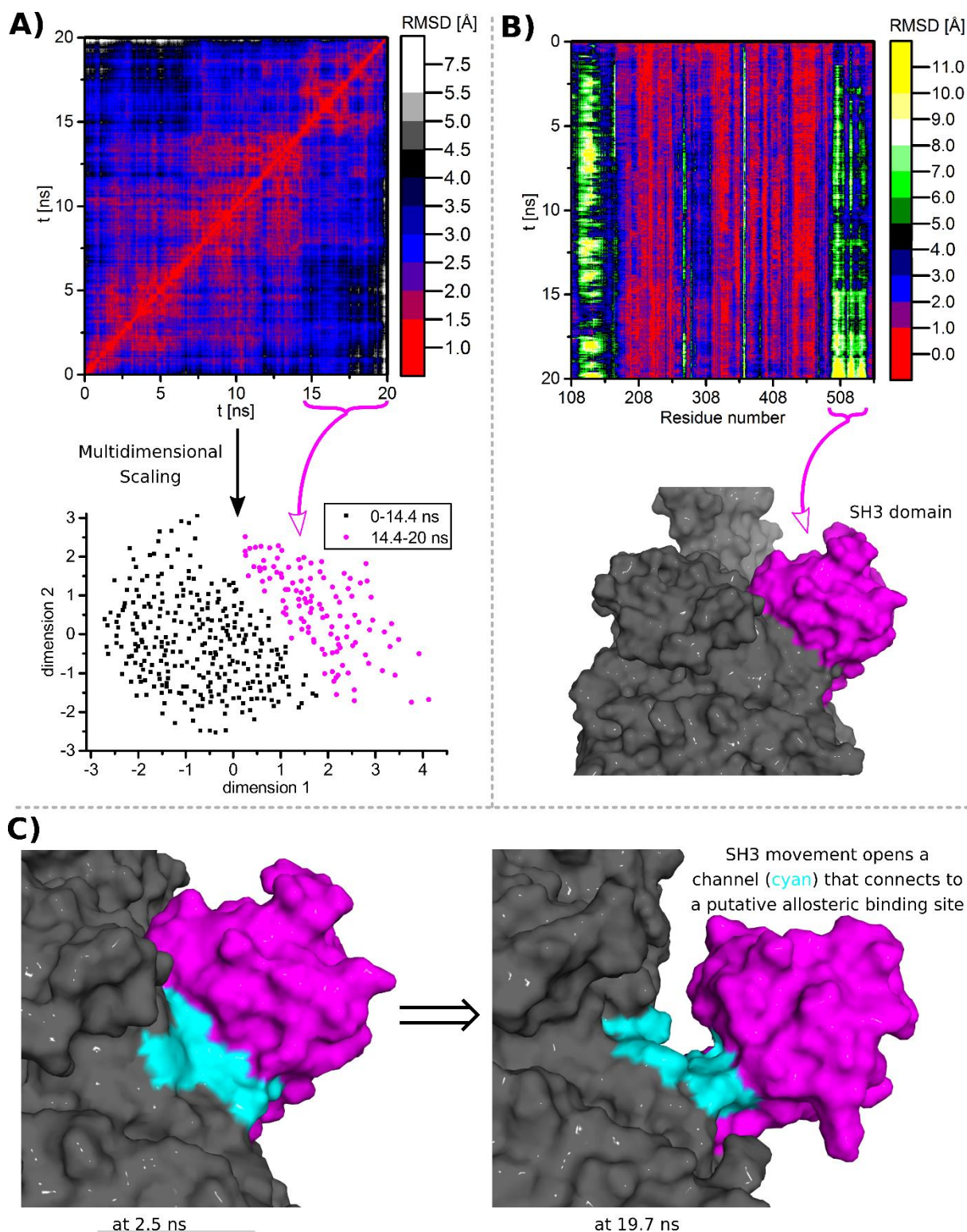


Figure 2. An MD simulation of FUT8 with a length of 20 ns was performed. A) An RMSD matrix (for all backbone atoms) of this MD simulation reveals a significant conformational change occurring after approximately 14.4 ns. Multidimensional scaling of this RMSD matrix highlights the conformational change in an easily comprehensible fashion. B) RMSD (of the C α -atom) of each residue (as referenced to the initial frame of the MD simulation) plotted against the simulation time. The plot reveals that the conformational change is caused by residues of the SH3 domain (colored in magenta). C) Two structures illustrate the previous findings: A significant snap back of the SH3 domain occurs. Interestingly, this movement opens a channel (colored in cyan) that connects to a putative allosteric binding site (cf. Fig. 3 and the associated paragraph)

For internal use, please do not delete. Submitted_Manuscript

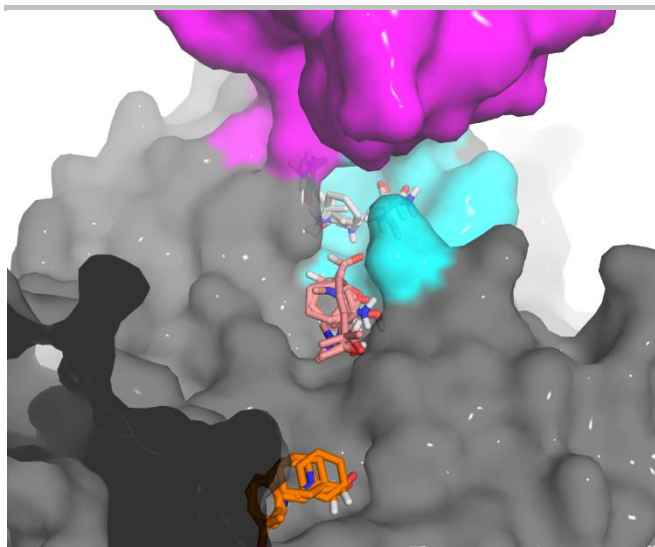


Figure 3. FTMap identifies four binding „hot spots“ on the back side (viewing from the acceptor site) of the channel (colored in cyan) that opens in the MD simulation. The MD-derived structure shown on the right side of panel C in Fig. 2 was used. This new putative binding site might be a target for inhibitor design and might offer specificity over other fucosyltransferases.

Design of a Ligand for the Donor Site:

For FUT8, the purine base and the pyrophosphate represent the structural proportions that dominantly contribute to the affinity of substrate binding.¹⁷⁻¹⁸ The other parts, i.e. the fucosyl residue and the heptasaccharide, exert specificity but little affinity. Therefore, we primarily focused on the design and synthesis of a donor site binder. At a later stage, we hope to link this donor site binder to structural proportions that are anchored in the new binding site described above and induce specificity by this. Therefore, we started a docking campaign against the donor site of FUT8. For this, we used the MD-derived structure shown in Fig. 4.

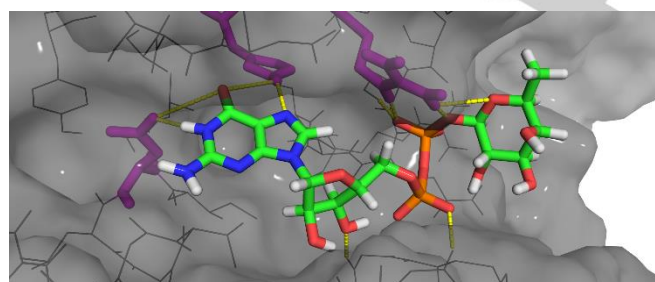


Figure 4. Binding mode of GDP-Fucose. Hydrogen bonds are shown in yellow. We hypothesized that three amino acid residues are of central significance for donor substrate binding: Asp-453, His-363, and Arg-365 (shown as magenta sticks).

We hypothesized that a potential ligand of the donor binding site should exhibit hydrogen bonding to three key amino acid residues: Asp-453, His-363, and Arg-365 (displayed as magenta sticks in Fig. 4). We ran two separate docking campaigns against the donor binding site of FUT8 employing a library of 700,000 fragments obtained from the ZINC12 database.²³ Two rather small grid boxes were used to ensure hits that cover the entire binding site. The grid box used in the first docking campaign was centered around the midpoint of the guanine moiety, the second centered on the β -phosphate (cf. supplement Fig. S2). In the first campaign, 1*H*-pyrazole-3,5-dicarboxamide **1**

(ZINC95830521) was identified as an interesting hit ranked second place in the docking hit list (see panel A in Fig. 5 for a binding pose, Tab. 1 for a short summary of docking results and supplement Tab. S2 for a longer hit list). The NH of the pyrazole moiety and a NH of the primary carboxamide function form pincer-like hydrogen bonding to Asp-453. The carbonyl oxygen of the second carboxamide function is able to hydrogen bond to His-363. In the second docking campaign, a large number of carboxylic acids hydrogen bonding to Arg-365 was identified with high docking scores (see supplement Tab. S3 for a hit list). In particular, 3,5-dihydroxyhydrocinnamic acid **2** (ZINC6091356) that was ranked 42nd place in the docking hit list caught our attention due to its structural simplicity and was subsequently exempt from one of the phenolic OH functions to yield 3-(3-hydroxyphenyl)propionic acid **3** (ZINC156346, see panel B in Fig. 5 for a binding pose). Both fragments, **1** and **3**, were linked *in silico* to yield ligand **4** (see panel C in Fig. 5 for a binding pose). This ligand showed an improved calculated binding energy compared GDP-Fucose in MM-GBSA calculations (see Tab. 1 for calculated binding energies). In order to reduce the synthetic effort, we decided to remove the phenolic OH function of **4**: Otherwise, protection of the phenolic OH group would have been inevitable and the synthesis of the corresponding building block would have started from 5-hydroxyisophthalic acid. The resulting ligand **5** (see panel D in Fig. 5 for a binding pose) still showed an improved calculated binding energy compared to GDP-Fuc (see Tab. 1). Importantly, ligand **5** exhibited stable hydrogen bonding to the three previously defined key amino acid residues (Asp-453, His-363, and Arg-365) during a MD simulation of a length of 1.5 ns.

Table 1. Docking scores (from GlideScore SP5.0) and calculated binding energies (from Prime MM-GBSA) for the donor substrate GDP-Fucose, docked fragments and ligands after *in silico* linking.

Ligand	Docking Score	MM-GBSA [kcal/mol]
GDP-Fuc	n.d.	-48.5
1	-6.116	-27.7
3	-6.413	-33.4
4	-9.182	-60.3
5	-8.363	-53.8

For internal use, please do not delete. Submitted_Manuscript

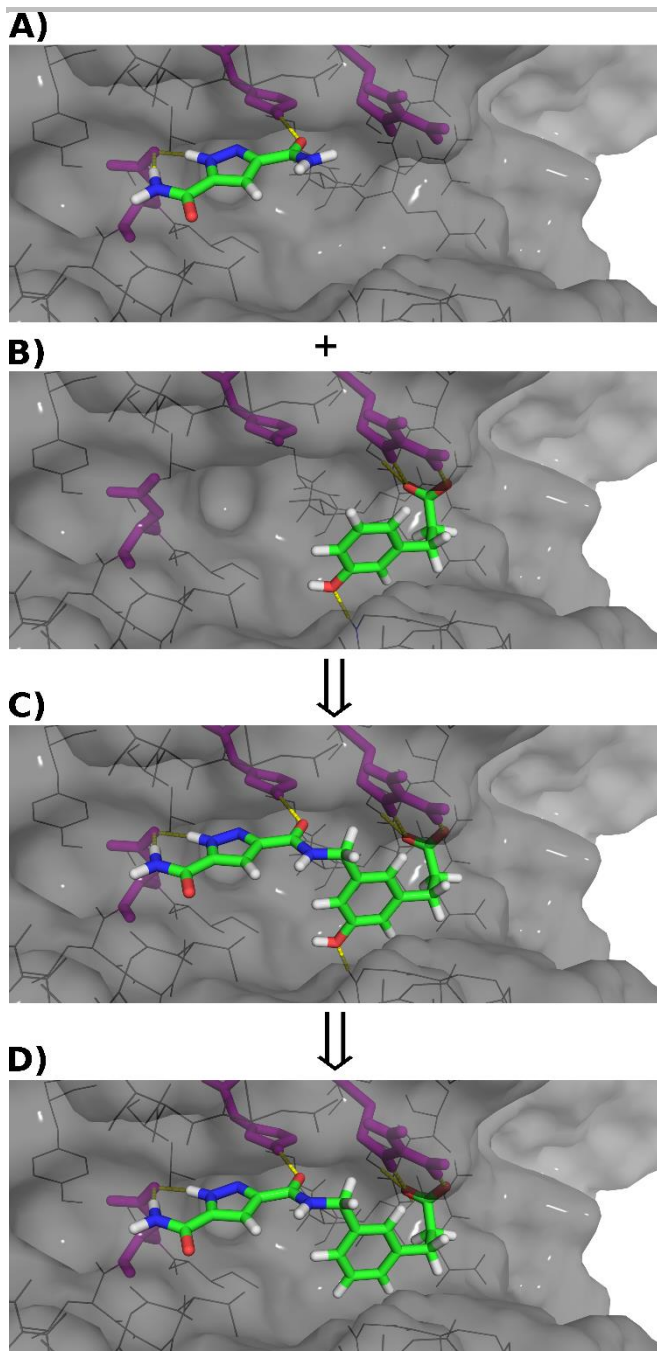


Figure 5. Docking a fragment library yielded the two fragments, **1** and **3** (panel A and B), that were subsequently linked *in silico* to yield ligand **4** (panel C). After exemption of the phenolic OH function ligand **5** (panel D) was obtained.

Synthesis of a Ligand for the Donor Site:

We envisioned a synthesis of ligand **5** by amide coupling of building blocks **6** and **7** and subsequent ester deprotection (see Fig. 6).

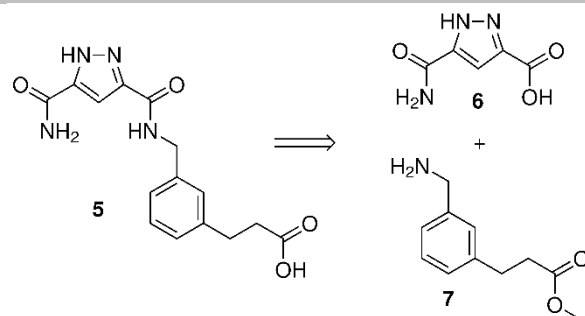


Figure 6. Retrosynthetic analysis of ligand **5**.

The synthesis of building block **6** was started from **8** which was accessed by employing a route similar to that described by Skinner *et al.*²⁴ The ester function of **8** was ammonolyzed to the primary amide **9** but in contrast to Skinner *et al.*,²⁴ who employed dry ammonia for this, we relied on a protocol by Jagdmann *et al.*²⁵ that releases ammonia by refluxing formamide in the presence of sodium methanoate. Finally, the aromatic methyl group of **9** was oxidized to give a carboxylic acid by the action of potassium permanganate.

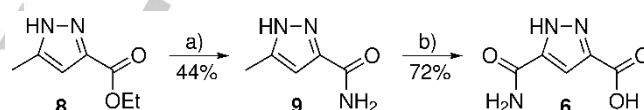


Figure 7. Synthesis of building block **6**. Reaction conditions: a) 4.0 eq. NaOMe, 6.0 eq. formamide, tetrahydrofuran, 5 h, 65 °C; b) 3.0 eq. KMnO₄, H₂O, 3 h, 95 °C.

Building block **7** is currently commercially available. We accessed **7** by a reaction sequence outlined in the supplement. Both building blocks, **6** and **7**, were subsequently linked via amide coupling using propylphosphonic anhydride as coupling reagent yielding **10**. Finally, the ester function of **10** was hydrolyzed by the action of potassium hydroxide to yield ligand **5**.

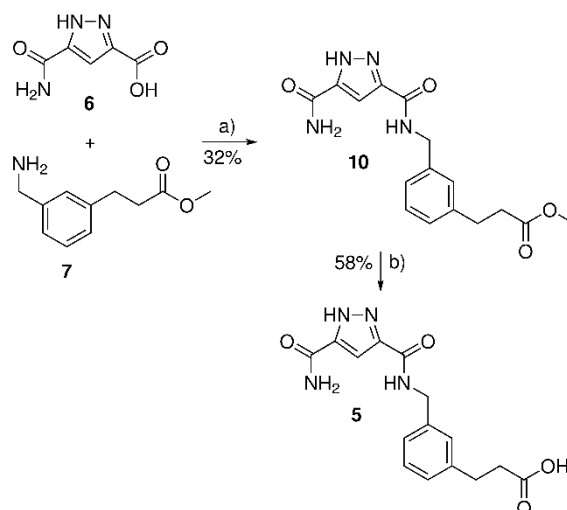


Figure 8. Synthesis of ligand **5**. Reaction conditions: a) 2.0 eq. DIPEA, 2.0 eq. propylphosphonic anhydride, DMF, 24 h, 20 °C; b) 3.0 eq. KOH, H₂O/MeOH 1:4, 24 h, 20 °C.

FULL PAPER

WILEY-VCH

Activity Assay:

We verified the functional activity of recombinantly expressed FUT8 by monitoring the fucosylation of 1- β -*N*-acetylchitotriose via $^1\text{H-NMR}$ spectroscopy over a course of 3.5 h. The progress of the reaction is visualized in Fig. 9. We derived initial rate constants from this period that are summarized in Tab. 2. Fucosylated 1- β -*N*-acetylchitotriose was produced with an apparent initial rate constant of 0.010 s^{-1} . This is in agreement with results of Ihara *et al.* who found a 5% activity for the core-fucosylation of chitotriose compared to the heptasaccharide *N*-glycan.²⁶

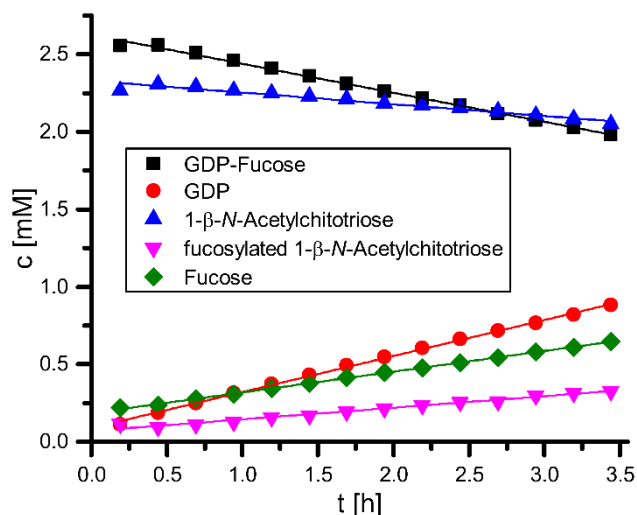


Figure 9. Activity assay for recombinantly expressed FUT8. The transfer of fucose from GDP-Fucose onto 1- β -*N*-acetylchitotriose was monitored via $^1\text{H-NMR}$ spectroscopy at 310 K.

Table 2. Initial rate constants for the depletion of GDP-Fucose and 1- β -*N*-acetylchitotriose and the production of GDP, fucosylated 1- β -*N*-acetylchitotriose and fucose.

	GDP-Fuc	GDP	Chitotriose	Fuc-Chitotriose	Fucose
$k_{\text{ini}} [\text{s}^{-1}]$	-0.026	0.032	-0.011	0.010	0.019

STD NMR:

Finally, we evaluated the dissociation constant for ligand **5**. STD NMR revealed a K_d of $1.65 \pm 0.97\text{ mM}$ (evaluating H-4'/H-6' (phenyl ring), see Fig. 10). A STD NMR spectrum acquired from a sample without added enzyme revealed no STD artefacts. Evaluation of the signal for the H-2' (phenyl ring) and H-4'' (pyrazole) yielded a higher K_d of 4.47 and 7.72 mM respectively. The signals of H-2 and H-3 (right next to the carboxy function) showed no STD effect. This is in accordance with the proposed binding mode in that all of the latter protons should be more solvent exposed than H-6'. Unfortunately, H-5' (phenyl ring) could not be evaluated because its signal is subsided by an impurity originating from the protein solution. Similarly, the benzyl protons could not be evaluated as they are strongly affected by water suppression.

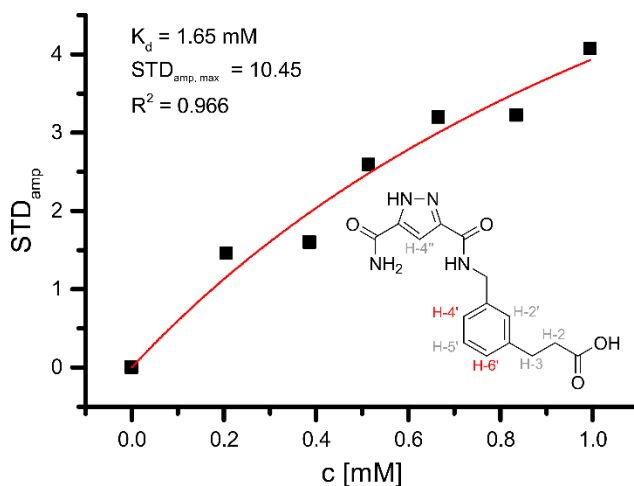


Figure 10. Determination of the dissociation constant of ligand **5** via STD NMR. The STD amplification factor of H-4'/H-6' (phenyl ring) is plotted against the concentration of **5**. As a result, by employing a one-site binding model the K_d of **5** was determined to be $1.65 \pm 0.97\text{ mM}$.

Results and Discussion

FUT8 has a very large and shallow binding site that is composed of the donor and the acceptor binding site. The acceptor binding site is known to stretch over five monosaccharide residues. It is very difficult to find inhibitors for such large and open binding sites. However, potent inhibitors of FUT8 are imperatively needed to clearly define its physiological role and might open new therapeutic avenues as well. We discussed a new putative binding site of FUT8 that can become accessible by a significant movement of the SH3 domain. An *in silico* analysis of this putative new binding site showed that a number of small fragments can bind to this area quite well. We expect a significant impact on future development of FUT8 inhibitors if this binding site can be verified experimentally: This putative binding site offers the prospect of adding specificity over other fucosyltransferases. Furthermore, we present a novel approach to generate inhibitors for FUT8 in that a fragment-based discovery process is utilized to discover new binders. For this, we performed a docking campaign with more than 700,000 fragments. The campaign yielded two interesting fragments. These two fragments were subsequently linked *in silico* and the binding of the resulting low-molecular weight ligand **5** was theoretically evaluated. Ligand **5** was synthesized and the corresponding dissociation constant was determined to 1.65 mM via STD NMR. Overall, the determined K_d is significantly higher than anticipated from MM-GBSA calculations (see section Ligand Design). This can be attributed to well-known shortcomings of MM-GBSA calculations. These include problems with entropic contributions and with charged ligands.²⁷ Even though we certainly hoped for a more affine ligand, we think that this molecule can be used as starting point for the development of inhibitors of FUT8 with drug-like properties. Taking the concept of ligand efficiency ($\text{LE} = -\Delta G/\text{no. of heavy atoms}$) into consideration,¹⁴ the presented ligand **5** features a ligand efficiency of $\text{LE} = 0.17$. In comparison, the most potent inhibitor of FUT8 known to date, reactive red 120 with a K_i of $2\ \mu\text{M}$,¹³ exhibits only a ligand efficiency of $\text{LE} = 0.09$ (due to its high molecular weight of $> 1.3\text{ kDa}$). Surely, an efficient binder should exhibit a $\text{LE} > 0.3$ but we take comfort in the fact that

For internal use, please do not delete. Submitted_Manuscript

potent inhibitors have emerged from low-affinity starting points before. For example, Chessari *et al.* reported the development of nanomolar inhibitors of cIAP1 starting from a fragment with an $IC_{50} > 5$ mM and a ligand efficiency of $LE < 0.21$.²⁸ We expect that in order to obtain specific inhibitors of FUT8 an extension of ligand **5** towards the acceptor binding site will be necessary. Even though a considerable enhancement of binding potency will be necessary in the ligand optimization process, we are confident that the expansion of this process will yield potent inhibitors of FUT8.

Experimental Section

Molecular Modeling:

We used Schrödinger's Maestro for molecular modeling. Schrödinger includes the software modules Prime, LigPrep, Glide, Desmond, and QikProp. The default force field is OPLS 2005.²⁹ On the basis of the only available X-ray crystal structure of human FUT8 (PDB: 2DE0) we recreated a model for donor substrate binding that has previously been developed in our working group.¹⁷ The FUT8-GDP-Fucose complex was taken to Desmond and fitted into an orthorhombic water box (SPC model) expanding 10 Å in each direction from the complex. Then, a 20 ns long MD simulation (Desmond v3) was performed using the NPT ensemble at 310 K. For the RMSD matrix (as shown in panel A of Fig. 2) every 100th structure (resulting in a total of 402 structures) of this MD simulation was exported to PyMol. All non-backbone atoms were deleted. Then, pairwise RMSD values for all structures were calculated by iterating PyMOL's "align" command with the cycles option set to zero employing a basic Python script. Multidimensional scaling of the resulting RMSD matrix was performed using Matlab's "mdscale" command using "sammon" as criterion and two dimensions. For the plot shown in panel B of Fig. 2, all atoms except C α -atoms were deleted. Then, structures were aligned to the initial frame of the MD simulation (employing PyMOL's "align" command with the cycles option set to zero). Finally, for the C α of each residue the RMSD value was calculated by employing PyMOL's "rms_cur" command. For the druggability assessment, the specified structure was uploaded to the FTMap server (<http://ftmap.bu.edu/serverhelp.php>).

We used the "FragmentsNow" subset of the ZINC12 databank for our docking campaigns. This library contains fragments with a molecular weight of less than 250 Da, a clogP of less than 3.5 and less than 5 rotatable bonds. This library was prepared at pH 7 \pm 0.2 using Maestro's LigPrep (with default options except pH) totaling about 700,000 ligands. Two independent docking campaigns were performed: The first one using a grid box centered around guanine (expanding 15, 17 and 17 Å in X, Y and Z direction) and the second one centered on the β -phosphate of GDP-Fuc (expanding 17 Å in X, Y, and Z direction, cf. supplement Fig. S2). Docking was performed using Glide (using default options). Initially the "HTVS" scoring function was used. Top hits were then redocked using the "Standard Precision" scoring function (GlideScore SP5.0). For MM-GBSA calculations, we used Prime (v3.0, OPLS3 force field). QikProp was used for calculations of log P values (QPlogPo/w is reported).

Synthesis:

5-Methyl-1*H*-pyrazole-3-carboxamide **9**: Synthesis was performed in accordance to a protocol by Jagdmann *et al.*²⁵ **8** (2.336 g, 15.15 mmol, 1.0 eq.) was dissolved in tetrahydrofuran (40 mL). Formamide (3.62 mL, 4.09 g, 90.9 mmol, 6.0 eq.) was added. Then, a 2.5 M solution of sodium methanoate (24.5 mL, 61.2 mmol, 4.0 eq.) in methanol was added. The reaction mixture was heated to reflux for 5 h and neutralized with dilute hydrochloric acid. Subsequently, the solvent was evaporated. The crude product was desalted by filtration over silica gel (eluent: dichloromethane/methanol 7:1). The residue was purified by column chromatography on silica gel (eluent: dichloromethane/methanol 7:1). **9** was obtained as a colorless solid (841 mg, 6.72 mmol, 44%). R_f : 0.23 (dichloromethane/methanol 7:1); ¹H-NMR (500 MHz, DMSO-*d*₆): δ [ppm] = 12.83 (s, 1H, NH), 7.37 (s, 1H, CONH₂), 7.10 (s, 1H, CONH₂), 6.37 (s, 1H, H-4), 2.22 (s, 3H, CH₃); ¹³C-NMR (126 MHz, DMSO-*d*₆): δ [ppm] = 163.8 (CONH₂), 146.9 (C-3), 139.7 (C-5), 104.2 (C-4), 10.4 (CH₃); HRMS (ESI⁺): expt. 148.0466 ([M+Na]⁺), calc. 148.0487 ([M+Na]⁺).

3-Carbamoyl-1*H*-pyrazole-5-carboxylic acid **6**. **9** (100 mg, 800 μ mol, 1.0 eq.) was suspended in water (10 mL). Potassium permanganate (379 mg, 2.40 mmol, 3.0 eq.) was added. The reaction mixture was stirred at 95 °C for 3 h and then filtrated while still hot. The filter cake was washed with hot water twice. The filtrate was treated with sodium sulfite until discoloration and then the pH value was adjusted to 1 with concentrated sulfuric acid. The solution was stored overnight at 4 °C during which product precipitated. The product was filtered off. **6** was obtained as a colorless solid (89 mg, 570 μ mol, 72%). ¹H-NMR (500 MHz, DMSO-*d*₆): δ [ppm] = 10.11 (bs, 2H, COOH, NH), 7.84 (s, 1H, CONH₂), 7.46 (s, 1H, CONH₂), 7.17 (s, 1H, H-4); ¹³C-NMR (126 MHz, DMSO-*d*₆): δ [ppm] = 161.6, 161.3 (CONH₂, COOH), 142.9, 140.0 (C-3, C-5), 108.3 (C-4); MS (ESI⁺): expt. 154.0174 ([M-H]⁻), calc. 154.0258 ([M-H]⁻).

Methyl 3-(3-((5-carbamoyl-1*H*-pyrazole-3-carboxamido)methyl)-phenyl)propanoate **10**. **6** (69 mg, 447 μ mol, 1.0 eq.) and **7** (95 mg, 492 μ mol, 1.1 eq.) were dissolved in *N,N*-dimethylformamide (2 mL). Then *N,N*-diisopropylethylamine (152 μ L, 116 mg, 894 μ mol, 2.0 eq.) was added and subsequently a solution of propylphosphonic anhydride (284 mg, 894 μ mol, 2.0 eq.) in *N,N*-dimethylformamide (50wt%, 522 μ L). The reaction mixture was stirred at room temperature for 24 h and then freed of the solvent *in vacuo*. The residue was taken up in 5% hydrochloric acid and extracted with ethyl acetate. The combined organic phases were dried over sodium sulfate, filtered and freed of the solvent *in vacuo*. The residue was purified via RP-HPLC (column: Nucleodur C₁₈ Isis; solvent A: 95% H₂O + 5% MeCN; solvent B: 95% MeCN + 5% H₂O; gradient: 0-5 min, 35% B; 5-13 min, 100% B; 13-15 min, 100% B; 15-18 min, 100% B; 18-20 min, 35% B; flow rate: 20 mL/min; R_t = 5.2 min). **10** was obtained as a colorless solid (51.5 mg, 156 μ mol, 32%). R_f : 0.37 (dichloromethane/methanol 9:1); ¹H-NMR (500 MHz, DMSO-*d*₆): δ [ppm] = 13.92 (bs, 1H, NH (pyrazole)), 8.88 (bs, 1H, R₁CONHCH₂R₂), 7.86 (bs, 1H, CONH₂), 7.44 (bs, 1H, CONH₂), 7.25 (s, 1H, H-4'), 7.23 (dd, 1H, ³J = 7.7 Hz, ³J = 7.7 Hz, H-5'), 7.16-7.14 (m, 1H, H-2'), 7.14-7.11 (m, 1H, ³J = 7.7 Hz, H-4'/H-6'), 7.10-7.07 (m, 1H, ³J = 7.5 Hz, H-4'/H-6'), 4.40 (d, 2H, ³J = 5.9 Hz, R₁CONHCH₂R₂), 3.56 (s, 3H,

COOCH₃), 2.83 (t, 2H, ³J = 7.6 Hz, H-3), 2.60 (t, 2H, ³J = 7.7 Hz, H-2); ¹³C-NMR (126 MHz, DMSO-*d*₆): δ [ppm] = 172.6 (COOCH₃), 140.5, 139.6 (C-1', C-3'), 128.3 (C-5'), 127.1 (C-2'), 126.6, 125.1 (C-4', C-6'), 105.7 (C-4''), 51.3 (COOCH₃), 41.9 (R₁CONHCH₂R₂), 34.8 (C-2), 30.2 (C-3); HRMS (ESI⁺): expt. 331.1360 ([M+H]⁺), calc. 331.1401 ([M+H]⁺).

3-(3-((5-Carbamoyl-1*H*-pyrazole-3-carboxamido)methyl)phenyl)propanoic acid **5**. **10** (41 mg, 124 μmol, 1.0 eq.) was dissolved in methanol (8 mL). Then, potassium hydroxide (21 mg, 372 μmol, 3.0 eq.) was dissolved in water (2 mL) and added to the solution described above. The reaction mixture was stirred at room temperature for 24 h and then neutralized with dilute hydrochloric acid. Subsequently, the solvent was evaporated. The residue was desalted by filtration over silica gel (eluent: dichloromethane/methanol 9:1 + 0.5% formic acid). The crude product was purified via RP-HPLC (column: Nucleodur C₁₈ Isis; solvent A: H₂O + 0.01% NH₃; solvent B: MeCN; gradient: 0-10 min, 10% B; 10-20 min, 40% B; 20-22 min, 90% B; 22-25 min, 90% B; 25-27 min, 10% B; 27-30 min, 10% B; flow rate: 1 mL/min; R_t = 5.0-7.0 min). **5** was obtained as a colorless solid (22.7 mg, 71.9 μmol, 58%). R_f: 0.17 (dichloromethane/methanol 9:1 + 0.5% formic acid); ¹H-NMR (500 MHz, DMSO-*d*₆): δ [ppm] = 8.95 (bs, 1H, R₁CONHCH₂R₂), 7.88 (bs, 1H, CONH₂), 7.42 (bs, 1H, CONH₂), 7.23 (s, 1H, H-4''), 7.21 (dd, 1H, ³J = 7.6 Hz, ³J = 7.6 Hz, H-5'), 7.17-7.15 (m, 1H, H-2'), 7.12-7.07 (m, 2H, H-4', H-6'), 4.40 (d, 2H, ³J = 6.1 Hz, R₁CONHCH₂R₂), 2.78 (t, 2H, ³J = 7.6 Hz, H-3), 2.43 (t, 2H, ³J = 7.6 Hz, H-2); ¹³C-NMR (126 MHz, DMSO-*d*₆): δ [ppm] = 174.5 (COOH), 161.3 (CONH₂), 160.1 (R₁CONHCH₂R₂), 141.5 (C-1'), 139.4 (C-3'), 128.2 (C-5'), 127.4 (C-2'), 126.6, 124.8 (C-4', C-6'), 105.8 (C-4''), 42.0 (R₁CONHCH₂R₂), 36.2 (C-2), 30.8 (C-3); HRMS (ESI⁺): expt. 315.1027 ([M-H]⁻), calc. 315.1093 ([M-H]⁻). Purity of **5** was determined from HPLC-MS (cf. supplement Fig. S12) to 96%.

Protein Expression:

The FUT8 cDNA was inserted into the baculovirus transfer vector pAcGP67B (BD Pharmingen, Heidelberg, Germany) and modified by addition of an N-terminal 10-fold His-tag, a V5 epitope, and a factor Xa cleavage site. *Spodoptera frugiperda* insect cells (Sf9) (Invitrogen) were grown at 27 °C in serum-free medium (SFX-Insect cell culture medium HyClone (GE Healthcare) containing 10 μg/ml gentamycin; Invitrogen). Recombinant baculovirus was generated by cotransfection of Sf9 cells with BaculoGold bright DNA (BD Pharmingen, Heidelberg, Germany) and the baculovirus transfer vector pAcGP67B containing FUT8. High titer stocks were produced by three rounds of virus amplification and optimal MOI for protein expression was determined empirically by infection of Sf9 cells in 6 well plates (1.0×10⁶ cells/well) with serial dilutions of high titer virus stock. The high titer stock of recombinant baculovirus was used to infect 500 mL suspension cultures of Sf9 cells (1.0×10⁶ cells per mL) in a roller bottle (850 cm² growth area, Greiner). For protein production, the cells were incubated at 27 °C and 110 rpm for 5 days. The supernatant of baculovirus-infected cells was collected, and applied to a nickel-chelating affinity matrix (HisTrap Excel, GE-Healthcare). The column was rinsed with binding buffer (50 mM sodium phosphate, pH 8, 500 mM NaCl) and pre-eluted with NTA binding buffer containing 20 mM imidazole. The recombinant protein was eluted from the matrix using NTA-binding buffer containing

300 mM imidazole. Purification was confirmed by SDS-PAGE and immunoblotting.

NMR experiments:

Activity assay and STD-NMR were measured on a Bruker Avance 700 MHz spectrometer in 3 mm NMR tubes. Samples were prepared in D₂O containing MES-*d*₃ (50 mM) and TMSP-*d*₄ (1 mM) at pD 7.0. The FUT8 solution was rebuffed to the buffer specified above by using Amicon Ultra-4 cellulose filter (molecular weight cut-off 5 kDa) and the protein concentration was determined by using a nanodrop at 280 nm.

Activity assay: The fucosylation of 1-β-*N*-acetylchitotriose was monitored via ¹H-NMR over a course of 3.5 h. Every 15 min a ¹H-NMR spectra with excitation sculpting was acquired at 310 K using a pseudo 2D pulse program. The first data point was acquired after 11.5 min. The sample contained a FUT8 concentration of 2 μM, a GDP-Fucose concentration of 2.6 mM and a 1-β-*N*-acetylchitotriose concentration of 2.3 mM. Additionally, the sample contained 10 U of alkaline phosphatase (EC 3.1.3.1) and 1 mg/mL bovine serum albumin. Spectra were acquired with 32,768 data points and a total of 64 scans. FIDs were multiplied with an exponential function (line broadening 0.2) before Fourier transformation. The concentration of assay components was determined from H-8 of GDP-Fuc and GDP, H-1 of (fucosylated) 1-β-*N*-acetylchitotriose and the H-6 methyl group of fucose.

STD NMR: The standard pulse program "stddiffesgp2d" was used. On resonance irradiation was applied at 0 ppm. Saturation was achieved by a cascade of 40 Gaussian pulses with a duration of 50 ms. To reduce the protein background a spinlock pulse of 15 ms length was used. Experiments were performed at 300 K. All samples contained a FUT8 concentration of 5 μM and ligand excesses of **5** ranging from 41 to 199. Spectra were acquired with 24,576 data points and a total of 512 scans. FIDs were multiplied with an exponential function (line broadening 2) before Fourier transformation. For the determination of dissociation constants STD amplification factors were plotted against the ligand concentration. The data points were then fitted using a one-site binding model in Origin2016G.

Keywords: Fragment-based drug discovery • Fucosyltransferase 8 • Glycosylation • Glycosyltransferase inhibitor • Molecular modeling

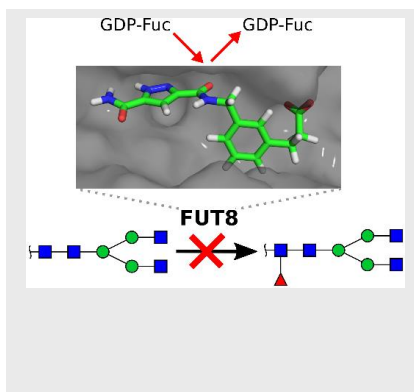
- [1] B. Ma, J. L. Simala-Grant, D. E. Taylor, *Glycobiology*, **2006**, *16*, 158-184.
- [2] R. L. Shields, J. Lai, R. Keck, L. Y. O'Connell, K. Hong, G. Meng, S. H. A. Weikert, L. G. Presta, L. G. *J. Biol. Chem.* **2002**, *277*, 26733-26740.
- [3] L. Malphettes, Y. Freyvert, J. Chang, P. Q. Liu, E. Chan, J. C. Miller, Z. Zhou, T. Nguyen, C. Tsai, A. W. Snowden, T. N. Collingwood, P. D. Gregory, G. J. Cost, *Biotechnol. Bioeng.* **2010**, *106*, 774-783.
- [4] P. Agrawal, B. Fontanals-Cirera, E. Sokolova, S. Jacob, C. A. Vaiana, D. Argibay, V. Davalos, M. McDermott, S. Nayak, F. Darvishian, M. Castillo, B. Ueberheide, I. Osman, D. Fenyö, L. K. Mahal, E. Hernandez, *Cancer Cell* **2017**, *31*, 804-819.
- [5] R. Honma, I. Kinoshita, E. Miyoshi, U. Tomaru, Y. Matsuno, Y. Shimizu, S. Takeuchi, Y. Kobayashi, K. Kaga, N. Taniguchi, H. Dosaka-Akita, *Oncology* **2015**, *88*, 298-308.

- [6] X. Wang, J. Chen, Q. K. Li, S. B. Peskoe, B. Zhang, C. Choi, E. A. Platz, H. Zhang, *Glycobiology* **2014**, *24*, 935-944.
- [7] X. Wang, S. Inoue, J. Gu, E. Miyoshi, K. Noda, W. Li, Y. Mizuno-Horikawa, M. Nakano, M. Asahi, M. Takahashi, N. Uozumi, S. Ihara, S. H. Lee, Y. Ikeda, Y. Yamaguchi, Y. Aze, Y. Tomiyama, J. Fujii, K. Suzuki, A. Kondo, S. D. Shapiro, C. Lopez-Otin, T. Kuwaki, M. Okabe, K. Honke, N. Taniguchi, *Proc. Natl. Acad. Sci. USA* **2005**, *102*, 15791-15796.
- [8] L. Tedaldi, G. K. Wagner, *Med. Chem. Commun.* **2014**, *5*, 1106-1125.
- [9] C. A. Lipinski, F. Lombardo, B. W. Dominy, P. J. Feeney, *Adv. Drug Deliv. Rev.* **2001**, *46*, 3-26.
- [10] Z. Tu, Y.-N. Lin, C.-H. Lin, *Chem. Soc. Rev.* **2013**, *42*, 4459-4475.
- [11] Y. Manabe, S. Kasahara, Y. Takakura, X. Yang, S. Takamatsu, Y. Kamada, E. Miyoshi, D. Yoshidome, K. Fukase, *Bioorg. Med. Chem.* **2017**, *25*, 2844-2850.
- [12] K. Hosoguchi, T. Maeda, J.-i. Furukawa, Y. Shinohara, H. Hinou, M. Sekiguchi, H. Togame, H. Takemoto, H. Kondo, S.-I. Nishimura, *J. Med. Chem.* **2010**, *53*, 5607-5619.
- [13] J. Kamińska, J. Dzieciol, J. Kościelak, *Glycoconj. J.* **1999**, *16*, 719-723.
- [14] A. L. Hopkins, G. M. Keserü, P. D. Leeson, D. C. Rees, C. H. Reynolds, *Nat. Rev. Drug Discov.* **2014**, *13*, 105-121.
- [15] A. D. Calderon, Y. Liu, X. Li, X. Wang, X. Chen, L. Li, P. G. Wang, *Org. Biomol. Chem.* **2016**, *14*, 4027-4031.
- [16] H. Ihara, Y. Ikeda, S. Toma, X. Wang, T. Suzuki, J. Gu, E. Miyoshi, T. Tsukihara, K. Honke, A. Matsumoto, A. Nakagawa, N. Taniguchi, *Glycobiology* **2007**, *17*, 455-466.
- [17] M. P. Kötzler, S. Blank, F. I. Bantleon, E. Spillner, B. Meyer, *Biochim. Biophys. Acta.* **2012**, *1820*, 1915-1925.
- [18] M. P. Kötzler, S. Blank, F. I. Bantleon, M. Wienke, E. Spillner, B. Meyer, *ACS Chem. Biol.* **2013**, *8*, 1830-1840.
- [19] J. B. Kruskal, *Psychometrika* **1964**, *29*, 1-27.
- [20] B. J. Mayer, *J. Cell Sci.* **2001**, *114*, 1253-1263.
- [21] D. Kozakov, D. R. Hall, R. L. Napoleon, C. Yueh, A. Whitty, S. Vajda, *J. Med. Chem.* **2015**, *58*, 9063-9088.
- [22] C. Mattos, D. Ringe, *Nature Biotechnol.* **1996**, *14*, 595-599.
- [23] J. J. Irwin, T. Sterling, M. M. Mysinger, E. S. Bolstad, R. G. Coleman, *J. Chem. Inf. Model.* **2012**, *52*, 1757-1768.
- [24] P. J. Skinner, M. C. Cherrier, P. J. Webb, Y.-J. Shin, T. Gharbaoui, A. Lindstrom, V. Hong, S. Y. Tamura, H. T. Dang, C. C. Pride, R. Chen, J. G. Richman, D. T. Connolly, G. Semple, *Bioorg. Med. Chem. Lett.* **2007**, *17*, 5620-5623.
- [25] G. E. Jagdmann, H. R. Munson, T. W. Gero, *Synth. Commun.* **1990**, *20*, 1203-1208.
- [26] H. Ihara, S. Hanashima, T. Okada, R. Ito, Y. Yamaguchi, N. Taniguchi, Y. Ikeda, *Glycobiology* **2010**, *20*, 1021-1033.
- [27] S. Genheden, U. Ryde, *Expert Opin. Drug Discov.* **2015**, *10*, 449-461.
- [28] G. Chessari, I. M. Buck, J. E. H. Day, P. J. Day, A. Iqbal, C. N. Johnson, E. J. Lewis, V. Martins, D. Miller, M. Reader, D. C. Rees, S. J. Rich, E. Tamanini, M. Vitorino, G. A. Ward, P. A. Williams, G. Williams, N. E. Wilsher, A. J.-A. Woolford, *J. Med. Chem.* **2015**, *58*, 6574-6588.
- [29] J. L. Banks, H. S. Beard, Y. Cao, A. E. Cho, W. Damm, R. Farid, A. K. Felts, T. A. Halgren, D. T. Mainz, J. R. Maple, R. Murphy, D. M. Philipp, M. P. Repasky, L. Y. Zhang, B. J. Berne, R. A. Friesner, E. Gallicchio, R. M. Levy, *J. Comp. Chem.* **2005**, *26*, 1752-1780.

Entry for the Table of Contents

FULL PAPER

Fucosyltransferase 8 catalyzes the core fucosylation of *N*-glycans. Here, we perform an *in silico* analysis of a new putative binding site of fucosyltransferase 8. Secondly, we describe the design and synthesis of a donor-site binder to start the development of inhibitors of fucosyltransferase 8 with drug-like properties.



Claas Strecker, Melissa Baerenfaenger, Michaela Mieke, Edzard Spiller, and Bernd Meyer*

Page No. – Page No.

In silico evaluation of the binding site of fucosyltransferase 8 and first attempts of synthesizing an inhibitor with drug-like properties